Annals of Nuclear Medicine
https://doi.org/10.1007/s12149-024-01969-7

ORIGINAL ARTICLE

How anatomical impairments found on CT affect perfusion percentage assessed by SPECT/CT scan?

Daniel M. Seraphim[1] · Katia H. Koga[2] · Antoine Vacavant[3] · Diana R. de Pina[2]

Received: 2 February 2024 / Accepted: 8 August 2024

Abstract

Aim CT images can identify structural and opacity alterations of the lungs while nuclear medicine's lung perfusion studies show the homogeneity (or lack of) of blood perfusion on the organ. Therefore, the use of SPECT/CT in lung perfusion scintigraphies can help physicians to assess anatomical and functional alterations of the lungs and to differentiate between acute and chronic disease.

Objective To develop a computer-aided methodology to quantify the total global perfusion of the lungs via SPECT/CT images and to compare these results with parenchymal alterations obtained in CT images.

Methods 39 perfusion SPECT/CT images collected retrospectively from the Nuclear Medicine Facility of Botucatu Medical School's Clinics Hospital in São Paulo, Brazil, were analyzed. Anatomical lung impairments (emphysema, collapsed and infiltrated tissue) and the functional percentage of the lungs (blood perfusion) were quantified from CT and SPECT images, with the aid of the free, open-source software 3D Slicer. The results obtained with 3D Slicer (3D-TGP) were also compared to the total global perfusion of each patient's found on their medical report, obtained from visual inspection of planar images (2D-TGP).

Results This research developed a novel and practical methodology for obtaining lungs' total global perfusion from SPECT/CT images in a semiautomatic manner. 3D-TGP versus 2D-TGP showed a bias of 7% with a variation up to 67% between the two methods. Perfusion percentage showed a weak positive correlation with infiltration ($p = 0.0070$ and $\rho = 0.43$) and collapsed parenchyma ($p = 0.040$ and $\rho = 0.33$).

Conclusions This research brings meaningful contributions to the scientific community because it used a free open-source software to quantify the lungs blood perfusion via SPECT/CT images and pointed that the relationship between parenchyma alterations and the organ's perfusion capability might not be so direct, given compensatory mechanisms.

Keywords Quantification · SPECT/CT · Lungs · 3D slicer · Nuclear medicine

Introduction

Chronic respiratory diseases (CRD), such as chronic obstructive pulmonary disease (COPD), are a leading cause of death worldwide, only behind cardiovascular conditions and neoplasms [1, 2]. Due to their high incidence and socio-economical impacts, prevention, control, and cure of respiratory diseases are among the most cost-effective health interventions available [3].

Imaging techniques, such as computed tomography (CT) and nuclear medicine's (NM) ventilation and perfusion (V/Q) lung scintigraphy provide noninvasive anatomical and functional information of the lungs. While CT images can identify structural and opacity alterations of the lungs (e.g., consolidation, bullae, atelectasis and interstitial disease),

✉ Diana R. de Pina
diana.pina@unesp.br

[1] Department of Structural and Functional Biology, Institute of Biosciences of Botucatu, Av. Professor Mário Rubens Guimarães Montenegro, S/N, UNESP Campus de Botucatu, Botucatu, SP CEP: 18618-687, Brazil

[2] Medical School, São Paulo State University Julio de Mesquita Filho, Av. Prof. Mário Rubens Guimarães Montenegro, S/N, UNESP Campus de Botucatu, Botucatu, SP CEP: 18618687, Brazil

[3] CNRS, SIGMA Clermont, IUT Clermont Auvergne, Pascal Institute, Clermont-Ferrand, F-63000 Clermont-Ferrand, France

Published online: 24 August 2024

NM's perfusion studies show the homogeneity (or lack of) of blood perfusion on the organ, associated with pulmonary emboli (PE), COPD, left ventricular heart failure, among others [4]. Therefore, these imaging techniques have been adopted as standard procedures in the diagnosis, staging and quantification of many pulmonary conditions [5, 6]. The combination of both modalities in hybrid equipment—SPECT/CT—has shown many benefits, including improvements in procedure planning that lead to better clinical outcome of patients [7–11]. More recently, CT also proved to be an essential tool for the diagnosis, follow-up and staging of COVID-19 [12], and V/Q SPECT/CT was used to assess functional alterations associated with lung lesions found these patients [13], with parenchymal lesions being responsible for V/Q injuries [14, 15].

These studies, however, relied on semi-quantitative visual inspection of SPEC/CT images. Although visual inspection is still the method of choice for identifying structural and functional impairment patterns, computer-aided quantification can be employed to assess the severity and extent of the findings [16–18]. Because discordant results may arise from visual and quantitative analyses of CT images, the combination of both methods is preferable in assessing and classifying impairments [19, 20]. Therefore, automatic (and semi-automatic) segmentation and quantification techniques are proving to be a valuable tool for assisting medical reports [21, 22] and, while they are being widely studied in radiology [23], there are still room for them to be explored in NM [24].

This work utilized retrospective lung perfusion SPECT/CT examinations to compute anatomical impairments found on CT image (emphysema, infiltrated and collapsed tissue) and compare them with the lung's perfusion percentage obtained from NM's scintigraphy. This was done with the aid of the free, open-source software 3D Slicer (www.slicer.org) [25], in a semiautomatic manner. Therefore, the objective of this study was to develop a new and practical methodology for obtaining lungs' total global perfusion from SPECT/CT images in a semiautomatic manner and to verify how structural impairments of the lungs, assessed bt CT images, impacted in its perfusion function, assessed by SPECT images.

Materials and methods

This study comprised two steps: the development of a methodology for segmenting and quantifying the SPECT/CT images and the application of the methodology on lung perfusion SPECT/CT images of a public university hospital database.

The study was duly approved by the institution's Research and Ethics Committee (CEP) under protocol CAEE 61704622.0.0000.5411. All clinical and patient data were obtained from the medical records. Because of the retrospective nature of this study, the need for informed consent was waived.

Database selection and characteristics

The algorithm was applied in a database comprised of lung perfusion SPECT/CT images obtained retrospectively in the Nuclear Medicine Facility of Botucatu Medical Schools Clinical Hospital in São Paulo, Brazil, over the period of 1 year (Jan 2021 to Jan 2022). The patients in the sample underwent the perfusion SPECT/CT examination to investigate chronic pulmonary embolism with and without pulmonary hypertension. The institution protocol for performing perfusion SPECT/CT do not include patients with fibrotic sequelae, interstitial pulmonary disease, and COPD. Figure 1 shows the flowchart of data selection and analysis.

A total of 54 examinations were analyzed. Inclusion criteria were procedures with both SPECT and CT sequences and medical report of normal or defective lung perfusion. Exclusion criteria were examinations that could not be retrieved from database, with missing medical report or medical report other than normal and defective perfusion (e.g., pulmonary shunt). The final database comprised of 39 examinations. Clinical data from these patients were also collected: age, sex, height, mass, medical report, total global perfusion (TGP) obtained from the medical report and pulmonary hypertension status obtained from the transthoracic echocardiography report. The administrated activity of ^{99m}Tc-labelled human albumin (^{99m}Tc-MAA) was registered too. The clinical aspects and radiopharmaceutical characteristics of the database are depicted in Table 1.

The SPECT/CT images were acquired in a Discovery NM/CT 670 scintillation camera (GE Healthcare, Milwaukee, WI) after the injection of ^{99m}Tc-MAA in supine position. SPECT image was acquired first, followed by CT. Then, both were processed in Xeleris 4 Workstation (GE Healthcare) to generate fused images. The acquisition and reconstruction parameters are presented in Table 2.

Segmentation and quantification algorithm

This study utilized 3D Slicer [25] version 4.11 in an Intel® Core™ i5-9300H based computer with 16 GB of RAM and 128 GB SSD to segment and quantify Digital Imaging and Communications in Medicine (DICOM) SPECT and CT images. First, images were imported into 3D Slicer for segmentation. In this step, the total anatomical volume of the lungs were obtained from the CT images, and the perfusion volume was obtained from the SPECT image with the aid of the anatomical information and radiopharmaceutical uptake. Then, these volumes were quantified

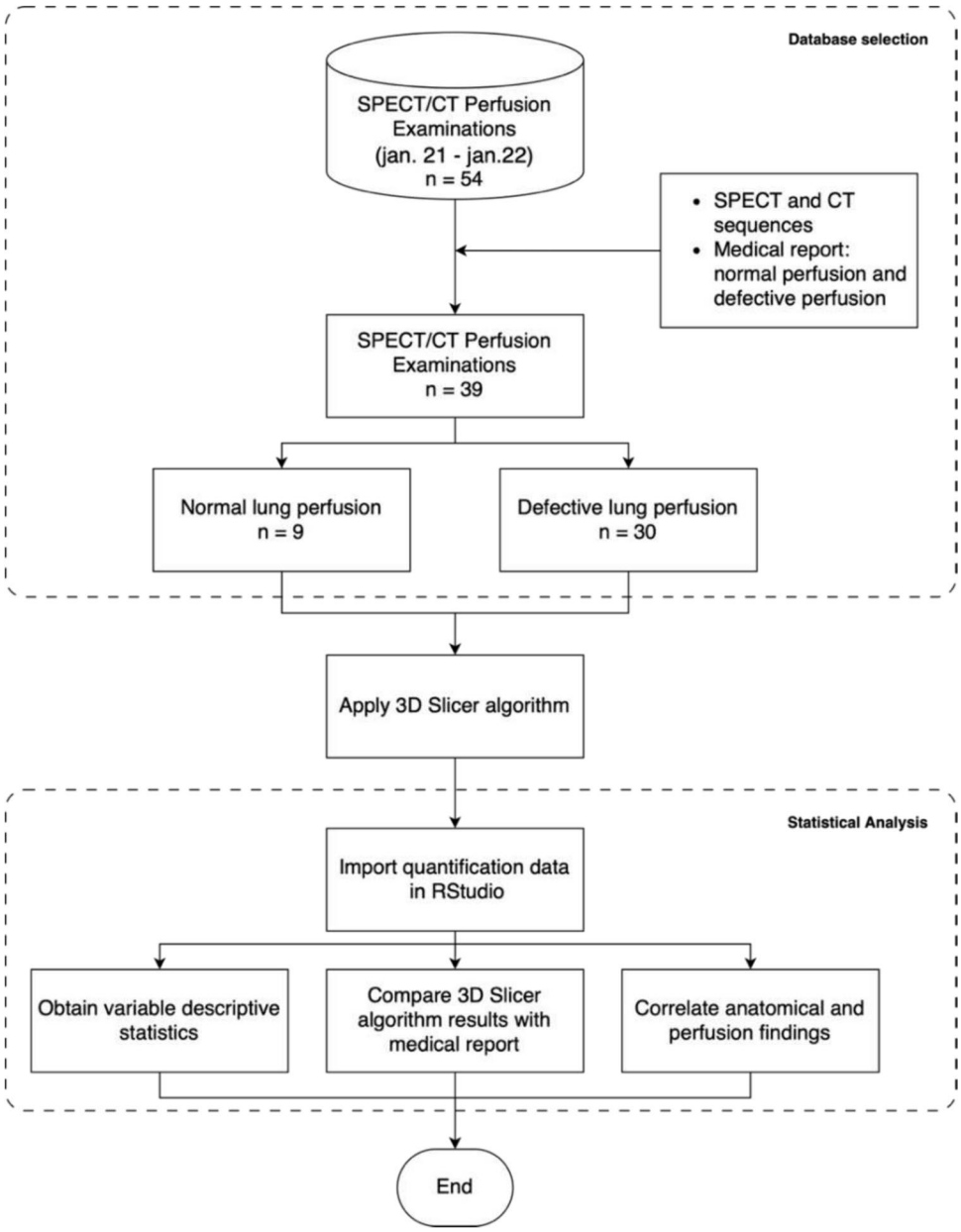

Fig. 1 Flowchart of database selection and statistical analysis

Table 1 Clinical and radiopharmaceutical characteristics of database per medical report group ($n=39$)

Characteristic	Normal perfusion ($n=9$) Median (range)	Defective perfusion ($n=30$) Median (range)
Age (years)	45 (18–67)	55 (25–78)
Sex	7 F | 2 M	18 F | 12 M
Mass (kg)	80 (57–126)	84 (52–126)
Height (cm)	162 (154–181)	163 (153–187)
BMI (kg/cm2)	31.22 (21.72–38.45)	30.15 (22.03–40.57)
Specific activity (MBq/kg)	3.43 (2.03–9.10)	3.93 (0.93–8.88)
Pulmonary Embolism	Excluded	Not excluded
Pulmonary Hypertension	Confirmed: 2 (22%) Mild (1) and Severe (1); Not confirmed: 7 (77%)	Confirmed: 4 (13%) Mild (1), Moderate (2) and Severe (1); Not confirmed: 18 (60%)

BMI Body mass index

Table 2 Acquisition and Reconstruction parameters of Perfusion SPECT/CT examination

Modality	Acquisition	Reconstruction
SPECT	Matrix: 128 × 128 pixels Projections: 120 Time/projection: 15 s Angular range: 360°	Iterative OSEM: 2 iterations, 4 subsets, Gaussian filter
CT	Scan type: Helical Voltage: 120 kV Current: 80–330 mA (Smart) Slice thickness: 5 mm Noise index: 11.5	Standard reconstruction, 5 mm, Lung filter

in cm3. The CT image was also used for assessing parenchymal alterations such: bullae/emphysema, infiltrated and collapsed tissue, and healthy, well-aerated parenchyma. Figure 2 depicts the workflow of the algorithm.

Anatomical segmentation of the lungs from CT images

CT images were processed in the *Lung Segmenter* plugin of the *Chest Imaging Plataform* (CIP) *(*Applied Chest Imaging Laboratory, Brigham and Women's Hospital, Boston, Massachusetts*)* to define the anatomical lung volume of interest (VOI). Once the lung VOIs were defined, the plugin *Lung Analyzer* was used to automatically identify and compute structural findings. This was done through Hounsfield Units (HU) thresholds [26–29]: bullae/emphysema (– 1.050 to – 950 HU); healthy parenchyma (– 950 to – 750 HU); infiltrated (– 750 to – 400 HU), which includes homogeneous lung opacities, such as ground glass opacity, consolidation and different types of pneumonia [30, 31]; besides collapsed (– 400 to 0 HU), associated with atelectasis. The total volume (cm3) of the lungs and of each finding was recorded.

Figure 3 depicts a visual example of the algorithm results: in (A) the coronal view of the lungs, in (B) the anatomical segmentation of the left and right lungs, and, in (C) the

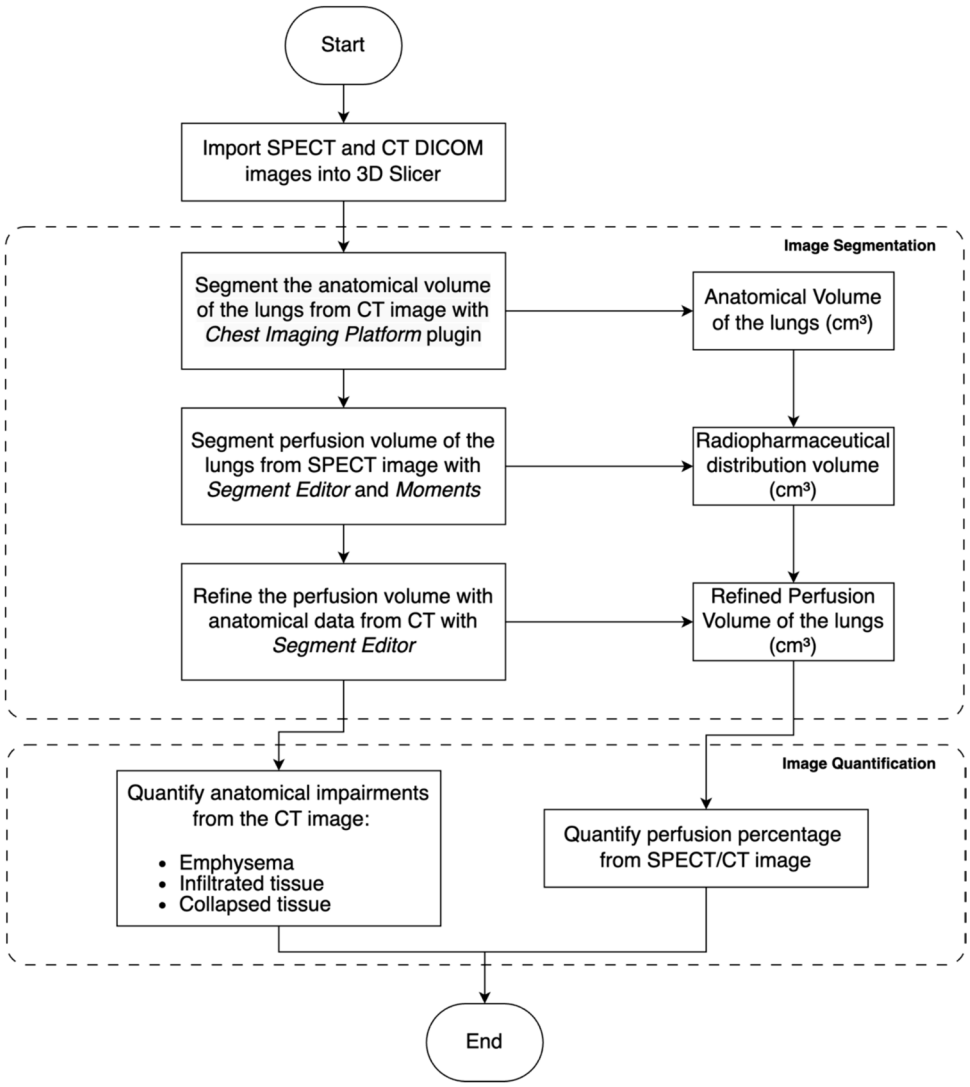

Fig. 2 Flowchart of algorithm segmentation and quantification

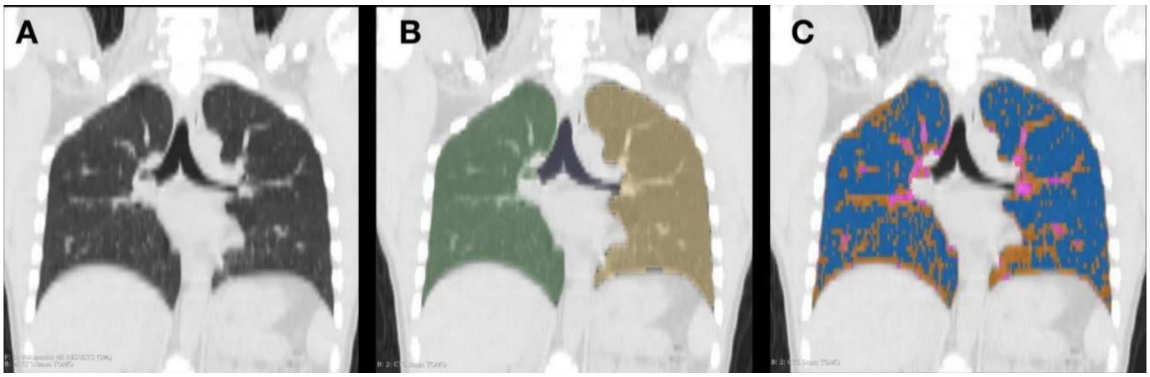

Fig. 3 Coronal views of the lungs (**a**), parenchymal segmentation (**b**) and anatomical impairments segmentation (**c**)

impairments masks show healthy (blue), infiltration (orange) and collapsed tissue (pink). Bullae/emphysema is not seen in this figure.

Segmentation of functional SPECT image

Once the anatomical volume of the lungs was obtained by CT, the SPECT image was segmented in the *Segment Editor* plugin of 3D Slicer. This process used an automatic threshold segmentation algorithm based on moment-preserving image segmentation analyses [32]. The lung VOI generated in Sect. 2.1.1 were used to limit the extension of the automatic generated perfusion volume—only pixels contained inside the anatomical region of the lungs were allowed to account for the perfusion segment. The volume (cm3) of the perfusion segments were obtained in the *Segment Statistics* plugin.

Figure 4 exemplifies the results of perfusion segmentation: in (A) the coronal view of the SPECT/CT fused image is shown, in (B) the outer (blue) mask represents anatomical segmentation of the lungs, as obtained from the algorithm described in Sect. 2.1.1., and the inner (yellow) mask represents the perfusion segmentation.

Figure 5 shows the software interface for segmenting the perfusion volume of the lungs. After the anatomical segmentation be completed, the organs volume can be used to refine the perfusion SPECT image, in the Segment Editor module. The blue shaded area represents the anatomical volume of the organ obtained from the CT image.

Quantification of anatomical impairments

The volume in cm3 of each impairment (bullae/emphysema, infiltrated and collapsed tissue) was divided by total volume of the lungs, also in cm3, to calculate the proportion of these findings that was present in the organ. According to the algorithm of CIP, affected lung was defined as the sum of emphysema, infiltrated, and collapsed volumes divided by the total volume of the lungs. On the other hand, healthy, well-aerated parenchyma, was defined as the portions of the lungs that were not affected (100% minus affected lung percentage).

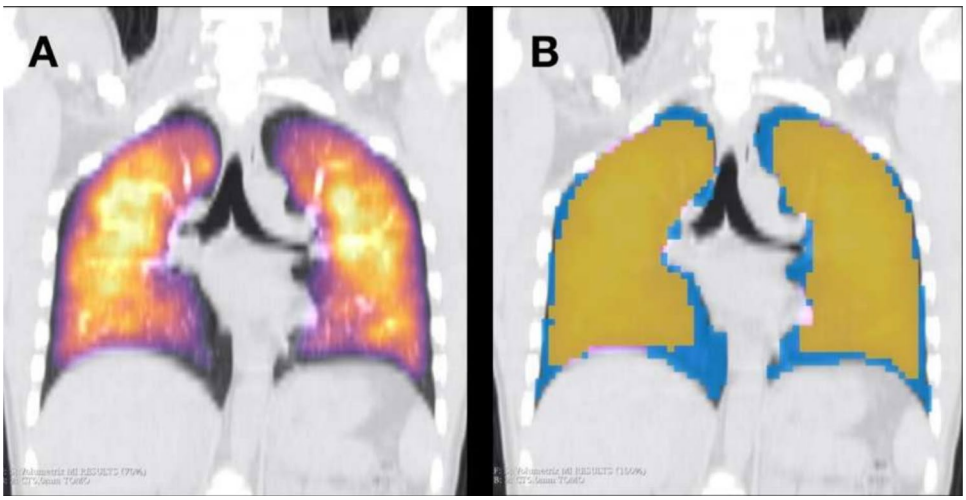

Fig. 4 Coronal views of SPECT/CT fused image (**a**) and anatomical (blue) and perfusion (yellow) segmentation (**b**) of a patient with normal lung perfusion

Fig. 5 Software interface for segmenting the perfusion volume of the lungs

Quantification of lung perfusion

The perfusion volume assessed by SPECT was compared to the anatomical volume of the lungs obtained from CT image to calculate the perfusion percentage of each patient. The absolute perfusion percentage was defined as perfusion volume divided by the total anatomical volume, in a similar fashion as the preserved lung perfusion function proposed by Xie et al. [18].

Statistical analysis

The percentage of each anatomical finding (bullae/emphysema, healthy, infiltrated and collapsed tissue) and the percentage of lung perfusion were used for statistical analysis. This analysis was performed in the free, open-source RStudio Software. Descriptive graphics, such as boxplots and scatter plots, were created to better visualize the distribution and correlation of the anatomical impairments and perfusion percentages. All these variables were also tested for normality through the Shapiro–Wilk test.

The distribution of the variables in both groups (normal and defective perfusion) was assessed to verify whether there were statistical differences between them. This was done through Student's t-Test for two independent samples with a confidence level of 95% and null hypotheses that the true difference in means for both groups were equal to zero.

Comparison of 3D Slicer results with medical report

The perfusion percentage obtained with this study's algorithm was compared with the perfusion percentage from each patient's medical report. The medical report perfusion percentage was assessed through a semi-quantitative visual inspection of six planar views of the lungs (anterior, posterior, both lateral and both posterior oblique views) and a score determination (0, 0.25, 0.5, 0.75, and 1) of the perfusion of each lobe [33], by two nuclear medicine specialists physicians comprising more than 20 years of experience. Results from both methods were compared through Bland–Altman analysis [34].

Correlation of anatomical and perfusion findings

Correlation tests were performed to assess the association of the perfusion percentage to: (a) inflated percentage, (b) bullae/emphysema percentage, (c) infiltrated percentage, (d) collapsed percentage and (e) total affected percentage. Both visual and analytical methods were employed to verify the relation among the variables.

Interpretation of correlation coefficients were: 0.9–1.0—very high correlation; 0.7–0.9—high correlation; 0.5–0.7—moderate correlation; 0.3–0.5—low correlation and 0.0–0.3—negligible correlation [35].

Results

Statistical analysis

Distribution of anatomical impairments are presented for both groups of patients—with normal and defective lung perfusion—in Fig. 6. Due to the low occurrence of emphysema in the sample (less than 1%), the scale of this graph was adjusted to better visualize its distribution. The difference in the mean value of each impairment between the normal and defective perfusion groups did not show significant statistical difference (p-value = 0.85 for infiltrated, p-value = 0.069 for collapsed and p-value = 0.24 for emphysema).

Figure 7 shows the distribution of affected and inflated lungs associated with impairments and healthy tissue, as assessed by CT. Since inflated percentage represents inverse information of affected lungs, the graphic shows complementary distribution.

With a p-value = 0.58 on Welch Two Sample t-Test, it is not possible to reject the null hypothesis, thus, the mean affected percentage is not different in defective and normal perfusion scans.

Figure 8 shows the total lung perfusion, or total global perfusion (TGP), obtained with the methodology of this study (3D-TGP) and data from the medical report of each patient (2D-TGP). 3D-TGP was calculated regarding total anatomical volume. With $p = 0.6462$ on Welch Two Sample t-Test for perfusion, it is not possible to reject the null hypothesis, thus, the mean perfusion on patients classified

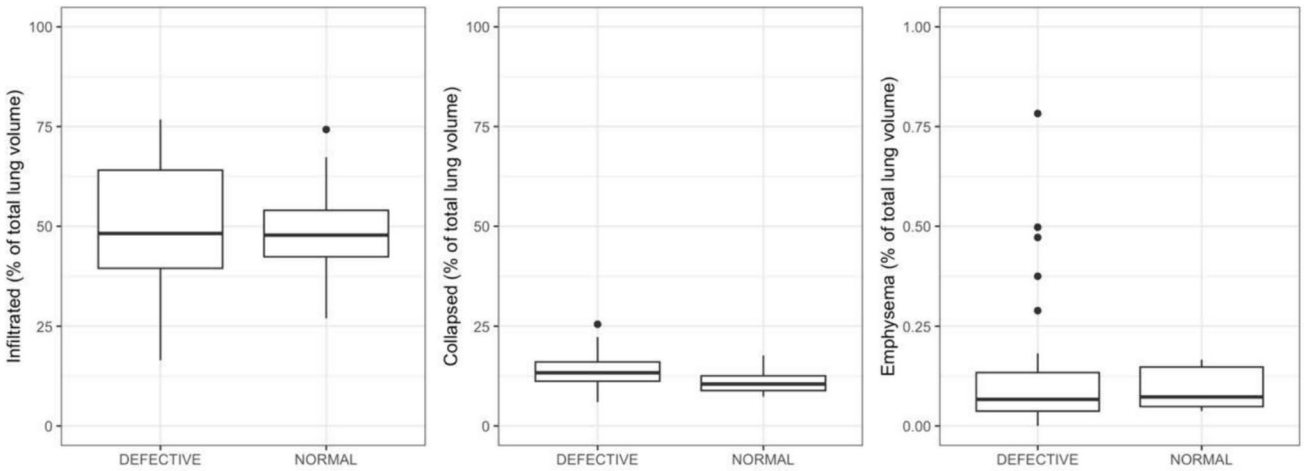

Fig. 6 Anatomical impairments obtained from CT per medical report: infiltrated (p-value = 0.85), collapsed (p-value = 0.069) and emphysema (p-value = 0.24) percentage

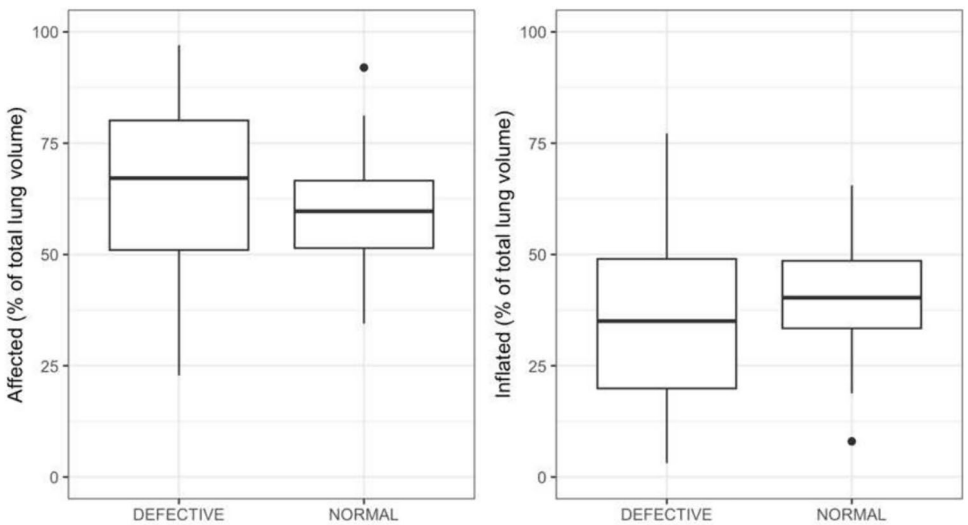

Fig. 7 Affected (p-value = 0.58) and inflated (p-value = 0.64) tissue assessed by CT per medical report

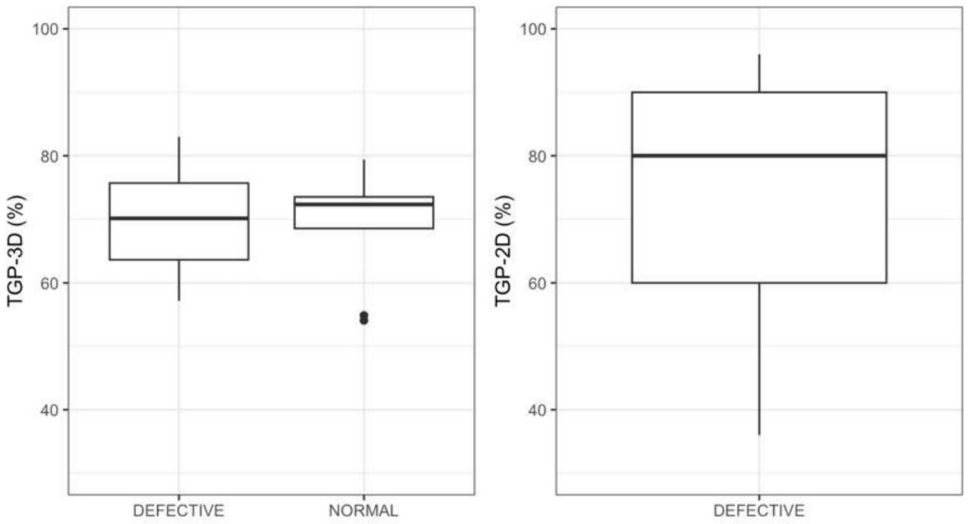

Fig. 8 Perfusion percentage obtained by SPECT (3D-TGP) and from the medical report (2D-TGP), by group

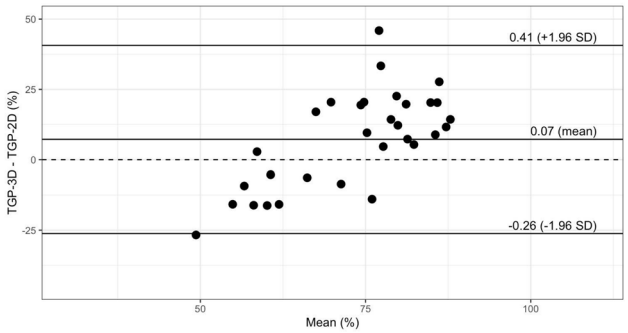

Fig. 9 Bland–Altman plot comparing total global perfusion obtained from medical report (2D-TGP) and the study's algorithm (3D-TGP)

with normal or defective perfusion shows no statistical difference. The defective perfusion group (DPG) presented higher variability in perfusion percentage than the normal perfusion group (NPG). On the other hand, NPG had slightly higher median perfused lung percentage (0.7231 versus 0.7012). Since the medical report did not include 2D-TGP for patients classified with normal lung perfusion, only the defective group is shown. The median value of 2D-TGP is 0.80.

Comparison of results from 3D Slicer with medical report

Figure 9 shows the Bland–Altman plot for 3D-TGP and 2D-TGP. 2D-TGP was obtained by visual inspection of planar images in a semi-quantitative mean from perfusion score of lung perfusion [33].

Since not all medical reports had the information of patient's TGP, the sample for this comparison was slightly smaller—comprising of 31 patients.

As can be seen, the plot shows no sign of systematic error between the two methods. On average, 3D-TGP is 7% greater than 2D-TGP and, from our sample, TGP could vary 67% from one method to the other (from the limits of agreement of -26% and 41%) [34].

Correlation of anatomical and perfusion findings

Finally, the correlation between variables was tested for both groups together, since no statistical difference was found in anatomical nor functional impairments distribution between them.

First, the correlation between individual anatomical impairments were tested through Spearman's correlation test. Infiltrated percentage of the lungs showed a weak positive correlation to the perfusion percentage ($p = 0.0070$ and $\rho = 0.43$), collapsed percentage showed an even weaker positive correlation ($p = 0.040$ and $\rho = 0.33$) and emphysema showed no correlation to perfusion percentage (p-value = 0.53). Figure 10 shows dispersion plots for each correlation assessment.

Then, perfusion percentage correlation to total affected percentage was tested. With $p = 0.0093$ and $\rho = 0.41$ in Spearman's rank correlation test, it is possible to assume that there is a positive correlation between the variables—even though it is weak. Figure 11 presents this result.

Discussion

The lack of statistical differences between both groups (normal and defective lung perfusion) regarding their perfusion percentage may be attributable to the low number of procedures available, especially on the normal perfusion group (30 deffective versus 9 normal). Nonetheless, the defective

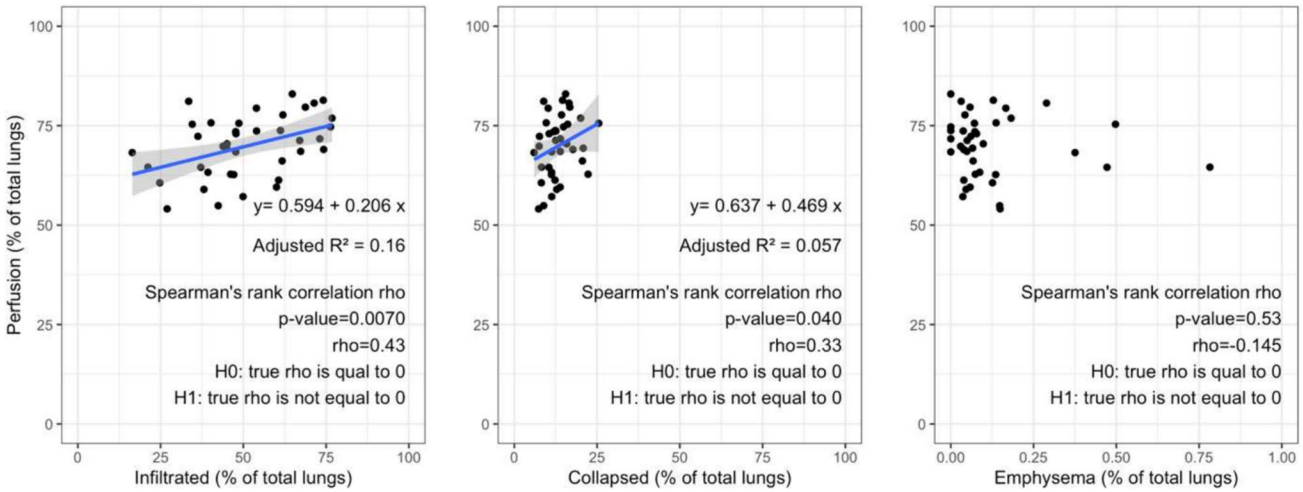

Fig. 10 Perfusion percentage (SPECT) versus anatomical impairment percentage (CT)

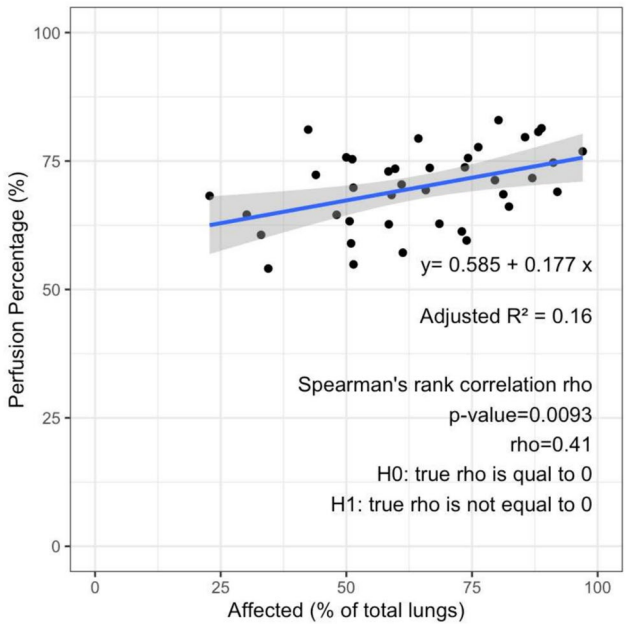

Fig. 11 Perfusion percentage (SPECT) versus total affected percentage (CT)

perfusion group showed a tendency of increased anatomical impairments findings, as can be seen on and Fig. 7, where the median of affected parenchyma is higher on the deffective than on the normal perfusion group (0.6716 versus 0.5971). A greater number of patients in both groups as well as a more even patient sample would be necessary to confirm this hypothesis.

The high percentage of infiltration found in the patients of our study (median of 0.4778) also raised awareness that other factor than patient lung disease was contributing to that. One hypothesis was that the radiopharmaceutical itself, due to its mechanism of capillary blockade [36], was responsible for increasing the mean HU number of the lung volume, leading to an overestimation of infiltrative and condensed tissue. Nonetheless, our study used optimal HU numbers for quantifying pulmonary parenchyma [29] and a prospective study would be required to clarify this hypothesis.

As can be seen in Fig. 9's Bland–Altman plot, TGP obtained with our methodology (3D-TGP) presented great variation when compared to TGP obtained from the medical report (2D-TGP). This result should come at no surprise since TGP were obtained from different types of images: planar and tomographic. Previous studies have shown significant differences when perfusion is quantified by planar or SPECT scintigraphy, with the later providing superior results [7, 37–39]. 3D SPECT images yields better anatomy assessment [40] and do not suffer from 'shine-through' effect from underlying normal perfusion areas, that can result in underestimation of perfusion defects [41]. Also, since our methodology utilized anatomical information from the CT scan to define the pulmonary volume, we believe that our results present a more trustworthy assessment of TGP.

Cobes et al. [13] found that anatomical impairments visible on CT scan from COVID-19 patients had a negative impact on the ventilatory capacity of the lungs, specially when ground glass opacity (infiltration) was present, while the perfusion remained mostly preserved. Evbuomwan et al. [42] observed areas with increased blood perfusion associated with inflamation on SPECT/CT studies and Bonnefey et al. [14] observed that consolidation in patients with COVID-19 was the most frequent and impactful injury to affect lung function. This is compatible with our findings, as can be seen in Fig. 10, where infiltration percentage of the parenchyma shows a positive correlation with blood perfusion percentage. This may be atribuited to the failure of the

hypoxic pulmonary vasoconstriction mechanism and presence of pulmonary thrombosis and emboli [15]. It should be noted that these works relied on semi-quantitative, visual inspection of SPECT/CT images whereas, in our study, this was done in a objective quantitavie manner.

Previous studies have also investigated the impact of emphysema on perfusion, and showed a negative correlation between these variables: the more emphysema the patient had, less perfusion was observed [43, 44]. The patients in our study, however, showed low degrees of emphysema involvment (less then 1% of the total lung volume), thus statistical analysis was inconclusive. This is reasonable when considering that the institution protocol for performing perfusion SPECT/CT do not include patients with fibrotic sequelae, interstitial pulmonary disease, and COPD.

Since the affected lung was defined as the sum of the individual impairments (emphysema, infiltration and collapsed), Fig. 11 shows its positive correlation with perfusion percentage. This is in acoordance with what has been reported in the literature, indicating that the methodology implied in this study yields to clinical plausible and relevant information, with less intra and interobserver variability.

Conclusion

This work developed a novel methodology to quantify the perfusion of the lungs from 3D SPECT/CT images through a free open-source software in a semiautomatic manner. The results obtained with 3D images can provide a more trustworthy assessment of the organ's blood perfusion when compared to the traditional visual inspection of planar images, since it reduces both human variability and geometric limitations imposed by 2D images. The study also used the software and the CT images to quantify anatomical impairments of the lungs and correlate them with its perfusion.

The algorithm proposed shows that 3D Slicer has the potential to be a valuable tool in clinical practice, since it applies semiautomatic analysis (less user dependent), does not require high end hardware and runs completely for free. The full process of segmentation and quantification of both anatomical and functional imaging took an average of 8.5 min where other studies have reported analysis time of 10–20 min [45].

This research brings meaningful contributions to the scientific literature because it: a) uses a free open-source software with few applications reported to date in nuclear medicine lung scans and b) compares structural to functional findings, highlighting that the relationtship between these two characteristics might not be so direct, given the action of compensatory mechanisms of the organism to maintain its viability.

Data availability The datasets generated and/or analyzed during the current study are not publicly available due to the privacy policy of our institution but are available from the corresponding author on reasonable request.

References

1. Soriano JB, Kendrick PJ, Paulson KR, Gupta V, Abrams EM, Adedoyin RA, et al. Prevalence and attributable health burden of chronic respiratory diseases, 1990–2017: a systematic analysis for the Global Burden of Disease Study 2017. Lancet Respir Med. 2020;8(6):585–96.
2. Sheikh K, Coxson HO, Parraga G. This is what COPD looks like. Respirology. 2016;21(2):224–36.
3. Forum of International Respiratory Societies., European Respiratory Society. The Global Impact of Respiratory Disease - Second Edition. Second. 2017.
4. Bajc M, Schümichen C, Grüning T, Lindqvist A, Le Roux PY, Alatri A, et al. EANM guideline for ventilation/perfusion single-photon emission computed tomography (SPECT) for diagnosis of pulmonary embolism and beyond. Eur J Nucl Med Mol Imaging. 2019;46(12):2429–51.
5. Welte T. Imaging in the diagnosis of lung disease. Dtsch Arztebl Int. 2014;111(11):179–80.
6. Jögi J, Markstad H, Tufvesson E, Bjermer L, Bajc M. The added value of hybrid ventilation/perfusion SPECT/CT in patients with stable COPD or apparently healthy smokers Cancer-suspected CT findings in the lungs are common when hybrid imaging is used. Int J COPD. 2014;10:25–30.
7. Toney LK, Wanner M, Miyaoka RS, Alessio AM, Wood DE, Vesselle H. Improved prediction of lobar perfusion contribution using technetium-99m-labeled macroaggregate of albumin single photon emission computed tomography/computed tomography with attenuation correction. J Thorac Cardiovasc Surg. 2014;148(5):2345–52.
8. Suh HY, Park S, Ryoo HG, Kim JY, Kim TS, Lee JM, et al. Comparative analysis of lung perfusion scan and SPECT/CT for the Evaluation of Functional Lung Capacity. Nucl Med Mol Imaging. 2019;53(6):406–13.
9. Si-Mohamed S, Moreau-Triby C, Tylski P, Tatard-Leitman V, Wdowik Q, Boccalini S, et al. Head-to-head comparison of lung perfusion with dual-energy CT and SPECT-CT. Diagn Interv Imaging. 2020;101(5):299–310.
10. Currie GM, Bailey DL. V/Q SPECT and SPECT/CT in pulmonary embolism. J Nucl Med Technol. 2023;51(1):9–15.
11. Romsa J, Imhoff RJ, Palli SR, Inculet R, Mehta S. SPECT/CT versus planar imaging to determine treatment strategy for non-small-cell lung cancer: a cost-effectiveness analysis. J Comp Eff Res. 2022;11(4):229–41.
12. Ufuk F, Savaş R. Chest CT features of the novel coronavirus disease (COVID-19). Turk J Med Sci. 2020;50(4):664–78.
13. Cobes N, Guernou M, Lussato D, Queneau M, Songy B, Bonardel G, et al. Ventilation/perfusion SPECT/CT findings in different lung lesions associated with COVID-19: a case series. Eur J Nucl Med Mol Imaging [Internet]. 2020;47:2453–60. https://doi.org/10.1007/s00259-020-04920-w.
14. Bonnefoy PB, Bahloul A, Denizot B, Barres B, Moreau-Triby C, Girma A, et al. Functional alterations due to COVID-19 lung lesions—lessons from a multicenter V/Q scan-based registry. Clin Nucl Med. 2022;47(8):e540–7.

15. Farkas B, Képes Z, Barna SK, Szugyiczki V, Bakos M, Forgács A, et al. Unusual perfusion patterns on perfusion-only SPECT/CT scans in COVID-19 patients. Ann Nucl Med. 2022;36(9):804–11.
16. Lynch DA, Austin JHM, Hogg JC, Grenier PA, Kauczor HU, Bankier AA, et al. CT-definable subtypes of chronic obstructive pulmonary disease: a statement of the fleischner society1. Radiology. 2015;277(1):192–205.
17. Nambu A, Zach J, Schroeder J, Jin G, Kim SS, Kim YIL, et al. Quantitative computed tomography measurements to evaluate airway disease in chronic obstructive pulmonary disease: Relationship to physiological measurements, clinical index and visual assessment of airway disease. Eur J Radiol. 2016;85(11):2144–51.
18. Xie H, Zhao Z, Zhang W, Li L. Quantitative analysis of lung function and airway remodeling using ventilation/perfusion single photon emission tomography/computed tomography and HRCT in patients with chronic obstructive pulmonary disease and asthma. Ann Nucl Med. 2023;37(9):504–16.
19. Barr RG, Berkowitz EA, Bigazzi F, Bode F, Bon J, Bowler RP, et al. A combined pulmonary-radiology workshop for visual evaluation of COPD: study design, chest CT findings and concordance with quantitative evaluation. COPD J Chronic Obstr Pulm Dis. 2012;9(2):151–9.
20. Park J, Hobbs BD, Crapo JD, Make BJ, Regan EA, Humphries S, et al. Subtyping COPD by using visual and quantitative CT imaging features. Chest. 2020;157(1):47–60.
21. Chan H, Hadjiiski LM, Samala RK. Computer-aided diagnosis in the era of deep learning. Med Phys. 2020;47(5):e218–27.
22. Binczyk F, Prazuch W, Bozek P, Polanska J. Radiomics and artificial intelligence in lung cancer screening. Transl Lung Cancer Res. 2021;10(2):1186–99.
23. Schalekamp S, Klein WM, van Leeuwen KG. Current and emerging artificial intelligence applications in chest imaging: a pediatric perspective. Pediatric Radiol. 2022;52:2120–30.
24. Hustinx R, Pruim J, Lassmann M, Visvikis D. An EANM position paper on the application of artificial intelligence in nuclear medicine. Eur J Nucl Med Mol Imaging. 2022;50(1):61–6.
25. Fedorov A, Beichel R, Kalpathy-Cramer J, Finet J, Fillion-Robin JC, Pujol S, et al. 3D Slicer as an image computing platform for the quantitative imaging network. Magn Reson Imaging. 2012;30(9):1323–41.
26. Berta L, De Mattia C, Rizzetto F, Carrazza S, Colombo PE, Fumagalli R, et al. A patient-specific approach for quantitative and automatic analysis of computed tomography images in lung disease: application to COVID-19 patients. Physica Med. 2021;82:28–39.
27. Risoli C, Nicolò M, Colombi D, Moia M, Rapacioli F, Anselmi P, et al. Different lung parenchyma quantification using dissimilar segmentation software: a multi-center study for COVID-19 Patients. Diagnostics. 2022;12(6):1501.
28. Wang Z, Gu S, Leader JK, Kundu S, Tedrow JR, Sciurba FC, et al. Optimal threshold in CT quantification of emphysema. Eur Radiol. 2013;23(4):975–84.
29. Ohkubo H, Kanemitsu Y, Uemura T, Takakuwa O, Takemura M, Maeno K, et al. Normal lung quantification in usual interstitial pneumonia pattern: The impact of threshold-based volumetric CT analysis for the staging of idiopathic pulmonary fibrosis. PLoS One. 2016;11(3):e0152505
30. Gotway MB, Reddy GP, Webb WR, Elicker BM, Leung JWT. High-resolution CT of the lung: patterns of disease and differential diagnoses. Radiol Cli N Am. 2005;43:513–42.
31. Patterson HS, Sponaugle DN. Is infiltrate a useful term in the interpretation of chest radiographs? Physician survey results Radiology. 2005;235:5–8.
32. Tsai WH. NOTE moment-preserving thresholding: a new approach. Vision. Graph Image Process. 1985;29:377–93.
33. Meyer G, Anne Collignon M, Guinet coise, Jeffreya AA, Barritault L. Comparison of perfusion lung scanning and angiography in the estimation of vascular obstruction in acute pulmonary embolism. Eur J Nucl Med. 1990;17(6–8):315–9.
34. Van Stralen KJ, Jager KJ, Zoccali C, Dekker FW. Agreement between methods. Kidney Int. 2008;74(9):1116–20.
35. Mukaka MM. Statistics corner: A guide to appropriate use of correlation coefficient in medical research. Malawi Med J. 2012;24(3):69–71.
36. Mettler FA, Guiberteau MJ. Respiratory system. In: Essentials of nuclear medicine and molecular imaging. Elsevier; 2019, p. 175–212. https://www.sciencedirect.com/book/9780323483193/essentials-of-nuclear-medicine-and-molecular-imaging#bookinfo.
37. Suh M, Kang YK, Ha S, Kim Y, Paeng JC, Cheon GJ, et al. Comparison of two different segmentation methods on planar lung perfusion scan with reference to quantitative value on SPECT/CT. Nucl Med Mol Imaging. 2017;51(2):161–8.
38. Phillips JJ, Straiton J, Staff RT. Planar and SPECT ventilation/perfusion imaging and computed tomography for the diagnosis of pulmonary embolism: A systematic review and meta-analysis of the literature, and cost and dose comparison. Eur J Radiol. 2015;84:1392–400.
39. Mazurek A, Dziuk M, Witkowska-Patena E, Piszczek S, Gizewska A. The utility of hybrid SPECT/CT lung perfusion scintigraphy in pulmonary embolism diagnosis. Respiration. 2015;90(5):393–401.
40. Knollmann D, Avondo J, Schaefer WM. Is hybrid SPECT/CT necessary for pre-interventional 3D quantification of relative lobar lung function? Eur J Hybrid Imaging. 2018;2(1):18.
41. Roach PJ, Bailey DL, Schembri GP, Thomas PA. Transition from planar to SPECT V/Q scintigraphy: Rationale, practicalities, and challenges. Semin Nucl Med. 2010;40:397–407.
42. Evbuomwan O, Engelbrecht G, Bergman MV, Mokwena S, Ayeni OA. Lung perfusion findings on perfusion SPECT/CT imaging in non-hospitalized de-isolated patients diagnosed with mild COVID-19 infection. Egypt J Radiol Nucl Med. 2021;52(1):144.
43. Suga K, Kawakami Y, Koike H, Iwanaga H, Tokuda O, Okada M, et al. Lung ventilation-perfusion imbalance in pulmonary emphysema: assessment with automated V/Q quotient SPECT. Ann Nucl Med. 2010;24(4):269–77.
44. Koike H, Sueyoshi E, Sakamoto I, Uetani M. Quantification of lung perfusion blood volume by dual-energy CT in patients with and without chronic obstructive pulmonary disease. J Belg Soc Radiol. 2015;99(1):62–8.
45. Kristiansen JF, Perch M, Iversen M, Krakauer M, Mortensen J. Lobar quantification by ventilation/perfusion SPECT/CT in patients with severe emphysema undergoing lung volume reduction with endobronchial valves. Respiration. 2019;98(3):230–8.